Inorg. Chem. **2004**, *43*, 3467−3474

Syntheses of Functionalized Ferratricarbadecaboranyl Complexes

Bhaskar M. Ramachandran, Patrick J. Carroll, and Larry G. Sneddon*

Department of Chemistry, University of Pennsylvania, Philadelphia, Pennsylvania 19104-6323

Received February 11, 2004

The reactions of nitriles (RCN) with *arachno*-4,6-$C_2B_7H_{12}^-$ provide a general route to functionalized tricarbadecaboranyl anions, 6-R-*nido*-5,6,9-$C_3B_7H_9^-$, R = C_6H_5 (**2**$^-$), $NC(CH_2)_4$ (**4**$^-$), (*p*-BrC_6H_4)(Me_3SiO)CH (**6**$^-$), $C_{14}H_{11}$ (**8**$^-$), and $H_3BNMe_2(CH_2)_2$ (**10**$^-$). Further reaction of these anions with (η^5-C_5H_5)$Fe(CO)_2I$ yields the functionalized ferratricarbadecaboranyl complexes 1-(η^5-C_5H_5)-2-C_6H_5-*closo*-1,2,3,4-$FeC_3B_7H_9$ (**3**), 1-(η^5-C_5H_5)-2-$NC(CH_2)_4$-*closo*-1,2,3,4-$FeC_3B_7H_9$ (**5**), 1-(η^5-C_5H_5)-2-[(*p*-BrC_6H_4)(Me_3SiO)CH]-*closo*-1,2,3,4-$FeC_3B_7H_9$ (**7**), 1-(η^5-C_5H_5)-2-$C_{14}H_{11}$-*closo*-1,2,3,4-$FeC_3B_7H_9$ (**9**), and 1-(η^5-C_5H_5)-2-$H_3BNMe_2(CH_2)_2$-*closo*-1,2,3,4-$FeC_3B_7H_9$ (**11**). Reaction of **11** with DABCO (triethylenediamine) resulted in removal of the BH_3 group coordinated to the nitrogen of the side chain, giving 1-(η^5-C_5H_5)-2-$NMe_2(CH_2)_2$-*closo*-1,2,3,4-$FeC_3B_7H_9$ (**12**). Crystallographic studies of complexes **3**, **5**, **7**, **9**, and **11** confirmed that these complexes are ferrocene analogues in which a formal Fe^{2+} ion is sandwiched between the cyclopentadienyl and tricarbadecaboranyl monoanionic ligands. The metals are η^6-coordinated to the puckered six-membered face of the tricarbadecaboranyl cage, with the exopolyhedral substituents bonded to the low-coordinate carbon adjacent to the iron.

Introduction

Because of their equivalent charges and formal electron donating abilities, the tricarbadecaboranyl (6-CH_3-*nido*-5,6,9-$C_3B_7H_9^-$)[1] (**1**$^-$) and cyclopentadienyl monoanions have been found to exhibit many similar transition metal coordination properties.[2] However, the resulting metallatricarbadecaboranyl complexes have significantly greater oxidative, chemical, thermal, and hydrolytic stabilities than their metallocene counterparts. Such differences have been exploited in the design of new active metallatricarbadecaboranyl analogues of established metallocene antitumor agents.[3] For example, cationic ferratricarbadecaboranyl [1-CpFe-2-CH_3-2,3,4-$C_3B_7H_9$]$^+X^-$ salts, like their ferrocenium counterparts, have now been shown to be effective cytotoxic agents, blocking growth in a number of culture lines.[4] More recently, we have designed and tested[5] a variety of new early metal tricarbadecaboranyl halide complexes that exhibit properties complementary to those of early-metal metallocene halide anticancer complexes.[3]

Previous studies of metallatricarbadecaboranyl complexes have generally employed only the 6-CH_3-*nido*-5,6,9-$C_3B_7H_9^-$ anion, but in order to achieve increased water solubility and/or specific binding properties, efficient routes are needed to generate functionalized complexes. The work described in this paper demonstrates that the reactions of a variety of nitriles with the *arachno*-4,6-$C_2B_7H_{12}^-$ monoanion provide a general route to tricarbadecaboranyl anions and complexes with chemically active substituents.

* Author to whom correspondence should be addressed. E-mail: lsneddon@sas.upenn.edu.

(1) Kang, S. O.; Furst, G. T.; Sneddon, L. G. *Inorg. Chem.* **1989**, *28*, 2339−2347.

(2) (a) Plumb, C. A.; Carroll, P. J.; Sneddon, L. G. *Organometallics* **1992**, *11*, 1665−1671. (b) Plumb, C. A.; Carroll, P. J.; Sneddon, L. G. *Organometallics* **1992**, *11*, 1672−1680. (c) Barnum, B. A.; Carroll, P. J.; Sneddon, L. G. *Organometallics* **1996**, *15*, 645−654. (d) Weinmann, W.; Wolf, A.; Pritzkow, H.; Siebert, W.; Barnum, B. A.; Carroll, P. J.; Sneddon, L. G. *Organometallics* **1995**, *14*, 1911−1919. (e) Barnum, B. A.; Carroll, P. J.; Sneddon, L. G. *Inorg. Chem.* **1997**, *36*, 1327−1337. (f) Müller, T.; Kadlecek, D. E.; Carroll, P. J.; Sneddon, L. G.; Siebert, W. *J. Organomet. Chem.* **2000**, *614*−*615*, 125−130. (g) Ramachandran, B. M.; Carroll, P. J.; Sneddon, L. G. *J. Am. Chem. Soc.* **2000**, *122*, 11033−11034. (h) Wasczcak, M. D.; Wang, Y.; Garg, A.; Geiger, W. E.; Kang, S. O.; Carroll, P. J.; Sneddon, L. G. *J. Am. Chem. Soc.* **2001**, *123*, 2783−2790. (i) Ramachandran, B. M.; Trupia, S. M.; Geiger, W. E.; Carroll, P. J.; Sneddon, L. G. *Organometallics* **2002**, *21*, 5078−5090.

(3) (a) Köpf-Maier, P.; Köpf, H. *Chem. Rev.* **1987**, *87*, 1137−1152. (b) Dombrowski, K. E.; Baldwin, W.; Sheats, J. E. *J. Org. Chem.* **1986**, *302*, 281−306. (c) Köpf-Maier, P.; Köpf, H. *Drugs Future* **1986**, *11*, 297−319. (d) Köpf-Maier, P.; Köpf, H. *Structure and Bonding*; Springer: Berlin, 1988; Vol. 70, pp 104−185.

(4) (a) Hall, I. H.; Warren, A. E.; Lee, C. C.; Wasczak, M. D.; Sneddon, L. G. *Anticancer Res.* **1998**, *18*, 951−962. (b) Wasczcak, M. D.; Hall, I. H.; Carroll, P. J.; Sneddon, L. G. *Angew. Chem., Int. Ed. Eng.* **1997**, *36*, 2227−2228.

(5) Hall, I. H.; Durham, R.; Tran, M.; Mueller, S.; Ramachandran, B. M.; Sneddon, L. G. *J. Inorg. Biochem.* **2003**, *93*, 125−131.

10.1021/ic049827a CCC: $27.50
Published on Web 04/29/2004

Table 1. NMR Data

compd	nucleus	δ [multiplicity, assignment, J (Hz)]
2$^-$	^{11}B[a,b]	8.1 (d, 1B, J_{BH} 144), 5.8 (d, 1B, J_{BH} 140), −4.0 (d, 1B, J_{BH} 148), −9.2 (d, 1B, J_{BH} 142), −12.4 (d, 1B, J_{BH} 144), −22.0 (d, 1B, J_{BH} 162), −28.0 (d, 1B, J_{BH} 145)
2	^{11}B[c,d]	26.9 (d, 1B, J_{BH} 167), 4.9 (d, 1B, J_{BH} 150), 2.8 (d, 1B, J_{BH} 161), −0.2 (d, 1B, J_{BH} 155), −3.9 (d, 1B, J_{BH} 176), −6.9 (d, 1B, J_{BH} 146), −30.1 (d, 1B, J_{BH} 164)
	^{1}H{^{11}B[d,e]}	7.44 (m, Ph), 7.24 (m, Ph), 6.97 (m, Ph), 3.94 (s, C9H, exo), 1.97 (s, C5H), −1.21 (s, C9H, endo)
	^{13}C[d,g]	157.56 (br, s, C6H), 130.84 (s, Ph), 128.81 (s, Ph), 128.52 (s, Ph), 57.24 (s, C4H), 30.16 (br, s, C9H$_2$)
4$^-$	^{11}B[a,b]	7.2 (d, 1B, J_{BH} 139), 4.9 (d, 1B, J_{BH} 136), −4.8 (d, 1B, J_{BH} 131), −10.0 (d, 1B, J_{BH} 145), −12.4 (d, 1B, J_{BH} 137), −23.8 (d, 1B, J_{BH} 158), −30.9 (d, 1B, J_{BH} 142)
4	^{11}B[c,d]	26.5 (d, 1B, J_{BH} 157), 5.3 (d, 1B, J_{BH} 149), 3.2 (d, 1B, J_{BH} 151), 0.1 (d, 1B, J_{BH} 156), −6.0 (d, 1B, J_{BH} 139), −6.6 (d, 1B, J_{BH} 122), −31.4 (d, 1B, J_{BH} 164)
	^{1}H{^{11}B[d,e]}	3.25 (s, C9H, exo), 1.85 (s, C5H), 1.30 (m, CH$_2$), 0.92 (m, CH$_2$), −1.52 (s, C9H, endo)
	^{13}C[d,g]	162.07 (br, s, C6H), 118.86 (s, CN), 61.16 (s, C4H), 32.30 (br, s, C9H$_2$), 28.60 (s, CH$_2$), 27.47 (s, CH$_2$), 26.29 (s, CH$_2$)
5	^{11}B[c,d]	2.2 (d, 1B, J_{BH} 158), −0.5 (d, 1B, J_{BH} 161), −8.9 (d, 1B, J_{BH} 141), −11.4 (d, 1B, J_{BH} 146), −25.4 (d, 1B, J_{BH} 151), −28.3 (d, 1B, J_{BH} 152), −32.5 (d, 1B, J_{BH} 157)
	^{1}H{^{11}B[d,e]}	6.60 (s, C3H), 3.92 (s, Cp), 2.81 (m, CH$_2$), 2.43 (m, CH$_2$), 1.54 (m, CH$_2$), 1.22 (m, CH$_2$), 0.81 (s, C4H)
7	^{11}B[c,d]	4.6 (d, 1B, J_{BH} 153), −1.2 (d, 1B[i]), −8.0 (d, 1B[h]), −11.0 (d, 1B[h]), −23.8 (d, 1B, J_{BH} 138), −27.6 (d, 1B, J_{BH} 149), −32.1 (d, 1B[h])
	^{1}H{^{11}B[d,e]}	7.34 (m, Ph), 6.41 (s, C3H), 4.18 (s, Cp), 1.83 (s, C4H), 0.0 (s, Me$_3$)
9	^{11}B[c,d]	7.5 (d, 1B, J_{BH} 150), 0.8 (d, 1B, J_{BH} 144), −3.9 (d, 1B, J_{BH} 147), −7.5 (d, 1B, J_{BH} 152), −19.8 (d, 1B, J_{BH} 143), −23.9 (d, 1B, J_{BH} 155), −28.8 (d, 1B, J_{BH} 148)
	^{1}H{^{11}B[d,e]}	7.85 (m, Ant), 7.33 (m, Ant), 7.18 (m, Ant), 7.04 (m, Ant), 6.57 (s, Ant, CH), 6.04 (s, C3H), 4.40 (d, Ant, CH$_2$), 4.16 (s, Cp), 3.63 (d, Ant, CH$_2$), 1.23 (s, C4H)
11	^{11}B[c,d]	3.4 (d, 1B, J_{BH} 145), −0.4 (d, 1B, J_{BH} 164), −9.3 (d, 1B, J_{BH} 136), −9.8 (m, 1B, J_{BH} 128), −10.9 (d, 1B, J_{BH} 130), −24.5 (d, 1B, J_{BH} 143), −27.6 (d, 1B, J_{BH} 158), −32.2 (d, 1B, J_{BH} 161)
	^{1}H{^{11}B[d,e]}	6.61 (s, C3H), 4.14 (s, Cp), 3.77 (m, CH$_2$), 3.61 (m, CH$_2$), 3.01 (m, CH$_2$), 2.79 (m, CH$_2$), 2.22 (s, Me), 2.08 (s, Me), 0.79 (s, C4H)
12	^{11}B[c,f]	2.3 (d, 1B, J_{BH} 156), −0.3 (d, 1B, J_{BH} 164), −8.8 (d, 1B, J_{BH} 144), −11.3 (d, 1B, J_{BH} 146), −25.3 (d, 1B, J_{BH} 146), −28.1 (d, 1B, J_{BH} 157), −32.2 (d, 1B, J_{BH} 155)
	^{1}H{^{11}B[e,f]}	6.80 (s, C3H), 4.75 (s, Cp), 3.78 (m, CH$_2$), 3.61 (m, CH$_2$), 3.28 (m, CH$_2$), 3.12 (m, CH$_2$), 1.99 (s, Me), 1.27 (s, Me), 0.88 (s, C4H)

[a] Glyme. [b] 64.2 MHz. [c] 160.5 MHz. [d] C_6D_6. [e] 500.1 MHz. [f] CD_2Cl_2. [g] 125.8 MHz. [h] The resonance was too broad to accurately measure the coupling constant.

Experimental Section

General Synthetic Procedures and Materials. Unless otherwise noted, all reactions and manipulations were performed in dry glassware under a nitrogen or argon atmosphere using the high-vacuum or inert-atmosphere techniques described by Shriver.[6]

The LiH, PhCN, NC(CH$_2$)$_4$CN, (*p*-BrC$_6$H$_4$)CHO, Me$_3$SiCN, ZnI$_2$, Me$_2$NCH$_2$CH$_2$CN, C$_{14}$H$_9$CN, 1.0 M HCl in Et$_2$O, (η^5-C$_5$H$_5$)-Fe(CO)$_2$I, and DABCO (triethylenediamine) were purchased from Strem or Aldrich and used as received. Spectrochemical grade glyme, Et$_2$O, toluene, CH$_3$CN, CH$_2$Cl$_2$, and hexanes were purchased from Fisher or EM Science. Glyme was freshly distilled from sodium−benzophenone ketyl prior to use. Acetonitrile was dried over P$_2$O$_5$, transferred onto activated 4 Å molecular sieves, and stored under vacuum. All other solvents were used as received unless noted otherwise.

Preparative thin-layer chromatography was conducted on 0.5 mm (20 × 20) silica gel F-254 plates (Merck-5744). The yields of all metallatricarbaborane products are calculated on the basis of starting metal reagents.

Physical Methods. The ^{11}B NMR at 64.2 MHz was obtained on a Bruker AC 200 Fourier transform spectrometer equipped with appropriate decoupling accessories. ^{11}B NMR at 160.5 MHz and ^{1}H NMR at 500.1 MHz were obtained on a Bruker AM-500 spectrometer equipped with the appropriate decoupling accessories. All ^{11}B chemical shifts are referenced to BF$_3$−O(C$_2$H$_5$)$_2$ (0.0 ppm), with a negative sign indicating an upfield shift. All proton chemical shifts were measured relative to internal residual protons from lock solvents (99.5% C_6D_6 and 99.9% CD_2Cl_2) and then referenced to (CH$_3$)$_4$Si (0.0 ppm). NMR data are given in Table 1.

High- and low-resolution mass spectra were obtained on a VG-ZAB-E high-resolution mass spectrometer. IR spectra were obtained on a Perkin-Elmer system 2000 FTIR spectrometer. Elemental analyses were obtained at the University of Pennsylvania microanalysis facility. Melting points were determined using a standard melting point apparatus and are uncorrected.

Syntheses of Li$^+$6-Ph-*nido*-5,6,9-C$_3$B$_7$H$_9^-$ (2$^-$) and 6-Ph-*nido*-5,6,9-C$_3$B$_7$H$_{10}$ (2). In a glovebag under nitrogen, 0.090 g (11.3 mmol, 0.95 equiv) of LiH and 1.34 g (11.9 mmol, 1.0 equiv) of *arachno*-4,6-C$_2$B$_7$H$_{13}$ were added to a two-neck, round-bottomed flask fitted with a stirbar, septum, and vacuum-connector/nitrogen-inlet. The flask was then connected to a vacuum line, and ∼20 mL of dry glyme was condensed into the flask at −196 °C. After stirring at room temperature for 45 min, the reaction mixture was filtered in a glovebag under nitrogen to remove any unreacted LiH. To the filtrate was added 10.0 mL (97.9 mmol) of PhCN, and the solution then was heated at reflux for 2 days under N$_2$. When ^{11}B NMR analysis indicated that the reaction was complete, the solution was filtered under N$_2$ and the solvent vacuum evaporated from the filtrate to give a yellow oily residue. Mass spectrometric analysis confirmed the presence of the 6-Ph-*nido*-5,6,9-C$_3$B$_7$H$_9^-$ (**2**$^-$) anion: HRMS (ES$^-$) calcd for ^{12}C$_9$^{1}H$_{14}$^{11}B$_7^-$ 198.1797, found 198.1787. The residue was dissolved in toluene to make a ∼0.5 M solution, which was then employed for the synthesis of the ferratricarbadecaboranyl complex 1-(η^5-C$_5$H$_5$)-2-C$_6$H$_5$-*closo*-1,2,3,4-FeC$_3$B$_7$H$_9$ (**3**), as described elsewhere.[2i] The exact concentration of the stock solution and the yield (74%) of **2**$^-$ were determined by integrating the resonances in the ^{11}B NMR spectrum of a B$_{10}$H$_{14}$ sample of known concentration, and comparing that value with the integrated value of the resonances of the stock solution.

To generate 6-Ph-*nido*-5,6,9-C$_3$B$_7$H$_{10}$ (**2**), a stirred solution of **2**$^-$, which was obtained by dissolving the crude product from above in 20 mL of methylene chloride, was reacted for 20 min at 0 °C with 12 mL of a 1 M solution of HCl in diethyl ether (12 mmol) (added slowly by syringe). With the reaction solution still maintained at 0 °C, the solvent was vacuum evaporated, leaving behind neutral 6-Ph-*nido*-5,6,9-C$_3$B$_7$H$_{10}$ (**2**). For **2**: crude yield (0.89 g, 4.4 mmol, 37%); HRMS calcd for ^{12}C$_9$^{1}H$_{15}$^{11}B$_7$ 200.1825, found 200.1835; mp ∼0 to −5 °C.

Syntheses of Li$^+$6-NC(CH$_2$)$_4$-*nido*-5,6,9-C$_3$B$_7$H$_9^-$ (4$^-$) and 6-NC(CH$_2$)$_4$-*nido*-5,6,9-C$_3$B$_7$H$_{10}$ (4). Using the concentrations and

(6) Shriver, D. F.; Drezdzon, M. A. *The Manipulation of Air-Sensitive Compounds*, 2nd ed.; Wiley: New York, 1986.

procedures described above, the *arachno*-4,6-$C_2B_7H_{12}^-$ anion was refluxed with 10.0 mL (88 mmol) of $NC(CH_2)_4CN$ to give an ~80% yield (again determined by NMR integration) of Li^+6-$NC(CH_2)_4$-*nido*-5,6,9-$C_3B_7H_9^-$. Mass spectrometric analysis confirmed the presence of the 6-$NC(CH_2)_4$-*nido*-5,6,9-$C_3B_7H_9^-$ (**4**$^-$) anion: HRMS (ES^-) calcd for $^{12}C_8{}^1H_{17}{}^{11}B_7{}^{14}N^-$ 204.2012, found 204.2009.

Acidification of **4**$^-$ using a procedure identical to that described for **2** gave the neutral 6-$NC(CH_2)_4$-*nido*-5,6,9-$C_3B_7H_{10}$ (**4**) in 31% yield (0.75 g, 3.7 mmol): HRMS calcd for $^{12}C_8{}^1H_{18}{}^{11}B_7{}^{14}N$ 205.2091, found 205.2088; mp ~0 to −5 °C.

Synthesis of 1-(η^5-C_5H_5)-2-$NC(CH_2)_4$-*closo*-1,2,3,4-$FeC_3B_7H_9$ (5). A toluene solution of **4**$^-$ (3.45 mL of 0.5 M, 1.7 mmol) was added dropwise to a stirring solution of (η^5-C_5H_5)$Fe(CO)_2I$ (0.523 g, 1.7 mmol) in THF (35 mL), resulting in a blue-green solution. After 12 h at room temperature, the mixture was opened to air and filtered and the dark filtrate evaporated to dryness. The residue was chromatographed on TLC plates (7:3 hexanes−CH_2Cl_2) to give a dark blue band (R_f 0.3) of 1-(η^5-C_5H_5)-2-$NC(CH_2)_4$-*closo*-1,2,3,4-$FeC_3B_7H_9$ (**5**) in 29% yield, (0.16 g, 0.49 mmol). For **5**: mp 111 °C. Anal. Calcd: C, 48.22; H, 6.85; N, 4.33. Found: C, 48.43; H, 7.03; N, 4.24. HRMS: calcd for $^{12}C_{13}{}^1H_{22}{}^{11}B_7{}^{14}N^{56}Fe$ 325.1753, found 325.1770. IR (KBr, cm^{-1}): 3111 (m), 2945 (s), 2865 (s), 2245 (m), 1706 (s), 1464 (s), 1421 (s), 1263 (s), 1210 (w), 1147 (w), 1116 (m), 1060 (w), 1012 (m), 967 (m), 935 (m), 837 (s), 817 (m).

Syntheses of Li^+6-[(*p*-BrC_6H_4)(Me_3SiO)CH]-*nido*-5,6,9-$C_3B_7H_9^-$ (6$^-$) and 1-(η^5-C_5H_5)-2-[(*p*-BrC_6H_4)(Me_3SiO)CH]-*closo*-1,2,3,4-$FeC_3B_7H_9$ (7). Using the concentrations and procedures described earlier, the *arachno*-4,6-$C_2B_7H_{12}^-$ anion was refluxed with 36.4 g (96 mmol) of [(*p*-BrC_6H_4)(Me_3SiO)CH]CN [prepared by room-temperature reaction of Me_3SiCN (5.0 g, 50.4 mmol) and (*p*-BrC_6H_4)CHO (9.32 g, 50.4 mmol) in the presence of catalytic amounts of ZnI_2 (2 mg)][7] for 4−5 days under N_2. After ^{11}B NMR analysis indicated consumption of the *arachno*-4,6-$C_2B_7H_{12}^-$, the solution was filtered under N_2 and the solvent vacuum evaporated from the filtrate to give a ~35% (1.2 g, 3.1 mmol) crude yield of the oily product. Mass spectrometric analysis confirmed the presence of the 6-[(*p*-BrC_6H_4)(Me_3SiO)CH]-*nido*-5,6,9-$C_3B_7H_9^-$ (**6**$^-$) anion: HRMS (ES^-) calcd for $^{12}C_{13}{}^1H_{23}{}^{11}B_7{}^{80}Br^{16}O^{28}Si^-$ 379.1353, found 379.1333.

The reaction of a toluene solution of **6**$^-$ (1.2 mL of 0.5 M, 0.6 mmol) with (η^5-C_5H_5)$Fe(CO)_2I$ (0.179 g, 0.6 mmol) in THF (35 mL) gave, following workup as described above for **5** and TLC separation (7:3 hexanes−CH_2Cl_2), a dark blue band (R_f 0.65) of 1-(η^5-C_5H_5)-2-[(*p*-BrC_6H_4)(Me_3SiO)CH]-*closo*-1,2,3,4-$FeC_3B_7H_9$ (**7**) in 22% yield (0.064 g, 0.13 mmol). For **7**: mp 161 °C. Anal. Calcd: C, 43.25; H, 5.65. Found: C, 43.35; H, 5.56. HRMS: calcd for $^{12}C_{18}{}^1H_{28}{}^{11}B_7{}^{80}Br^{56}Fe^{16}O^{28}Si$ 500.1094, found 500.1115. IR (KBr, cm^{-1}): 3106 (s), 3053 (m), 2963 (s), 2925 (s), 2854 (s), 2363 (w), 2270 (w), 2050 (w), 1944 (w), 1907 (m), 1783 (m), 1701 (w), 1589 (s), 1485 (s), 1447 (m), 1403 (w), 1376 (w), 1261 (s), 1191 (w), 1096 (s), 931 (w), 801 (s).

Syntheses of Li^+6-$C_{14}H_{11}$-*nido*-5,6,9-$C_3B_7H_9^-$ (8$^-$) and 1-(η^5-C_5H_5)-2-$C_{14}H_{11}$-*closo*-1,2,3,4-$FeC_3B_7H_9$ (9). Following the procedures described earlier, the *arachno*-4,6-$C_2B_7H_{12}^-$ anion was refluxed with 11.0 g (54 mmol) of $C_{14}H_9CN$ for 4−5 days under N_2. After ^{11}B NMR analysis indicated consumption of the *arachno*-4,6-$C_2B_7H_{12}^-$, the solution was filtered under N_2 and the solvent vacuum evaporated from the filtrate to give a ~15% (0.4 g, 1.3 mmol) crude yield of the oily product. Mass spectrometric analysis confirmed the presence of the 6-$C_{14}H_{11}$-*nido*-5,6,9-$C_3B_7H_9^-$ (**8**$^-$) anion: HRMS (ES^-) calcd for $^{12}C_{17}{}^1H_{20}{}^{11}B_7^-$ 301.2216, found 301.2201.

The reaction of a toluene solution of **8**$^-$ (2.4 mL of 0.5 M, 1.2 mmol) with (η^5-C_5H_5)$Fe(CO)_2I$ (0.365 g, 1.2 mmol) in THF (35 mL) gave, following workup as described above for **5** and TLC separation (CH_3CN), a dark blue band (R_f 0.6) of 1-(η^5-C_5H_5)-2-$C_{14}H_{11}$-*closo*-1,2,3,4-$FeC_3B_7H_9$ (**9**) in 8.5% yield (0.043 g, 0.10 mmol). For **9**: mp 184 °C. Anal. Calcd: C, 62.77; H, 5.99. Found: C, 62.90; H, 5.99. HRMS: calcd for $^{12}C_{22}{}^1H_{25}{}^{11}B_7{}^{56}Fe$ 422.1957, found 422.1987. IR (KBr, cm^{-1}): 3110 (s), 3048 (m), 3027 (s), 2929 (s), 2872 (s), 2821 (s), 2800 (m), 2361 (w), 2262 (w), 1987 (m), 1812 (w), 1607 (m), 1575 (m), 1487 (s), 1448 (s), 1421 (s), 1363 (s), 1351 (m), 1325 (w), 1282 (m), 1257 (m), 1237 (w), 1204 (w), 1173 (m), 1154 (m), 1118 (s), 1043 (w), 1013 (w), 1004 (w), 974 (m), 936 (m), 922 (m), 900 (w), 865 (m).

Syntheses of Li^+6-$H_3BNMe_2(CH_2)_2$-*nido*-5,6,9-$C_3B_7H_9^-$ (10$^-$) and 1-(η^5-C_5H_5)-2-$H_3BNMe_2(CH_2)_2$-*closo*-1,2,3,4-$FeC_3B_7H_9$ (11). Following the procedures described earlier, the *arachno*-4,6-$C_2B_7H_{12}^-$ anion was refluxed with 5.0 mL (44 mmol) of $Me_2NCH_2CH_2CN$ for 4−5 days under N_2. After ^{11}B NMR analysis indicated consumption of the *arachno*-4,6-$C_2B_7H_{12}^-$, the solution was filtered under N_2 and the solvent vacuum evaporated from the filtrate to give a ~17% (0.3 g, 1.5 mmol) crude yield of an oily product. Mass spectrometric analysis confirmed the presence of the 6-$H_3BNMe_2(CH_2)_2$-*nido*-5,6,9-$C_3B_7H_9^-$ (**10**$^-$) anion**:** LRMS (ES^-) calcd for $^{12}C_7{}^1H_{22}{}^{11}B_8{}^{14}N^-$ 208, found 208.

The reaction of a toluene solution of **10**$^-$ (2.2 mL of 0.5 M, 1.1 mmol) with (η^5-C_5H_5)$Fe(CO)_2I$ (0.314 g, 1.1 mmol) in THF (35 mL) gave, following workup as described above for **5** and TLC separation (CH_3CN), a dark blue band (R_f 0.4) of 1-(η^5-C_5H_5)-2-$H_3BNMe_2(CH_2)_2$-*closo*-1,2,3,4-$FeC_3B_7H_9$ (**11**) in 7% yield (0.022 g, 0.70 mmol). For **11**: mp 143 °C. Anal. Calcd: C, 43.99; H, 8.30; N, 4.27. Found: C, 43.25; H, 8.29; N, 4.28. HRMS: calcd for $^{12}C_{12}{}^1H_{27}{}^{11}B_8{}^{14}N^{56}Fe$ 329.2237, found 329.2234. IR (KBr, cm^{-1}): 3306 (s), 3113 (m), 3035 (m), 2956 (s), 2854 (m), 2360 (w), 2118 (m), 1608 (w), 1458 (w), 1418 (w), 1364 (m), 1275 (m), 1217 (w), 1150 (w), 1113 (m), 1050 (m), 1015 (w), 976 (w), 865 (m), 846 (m).

Reaction of 11 with Triethylenediamine (DABCO): Synthesis of 1-(η^5-C_5H_5)-2-$NMe_2(CH_2)_2$-*closo*-1,2,3,4-$FeC_3B_7H_9$ (12). A 0.03 mmol (0.010 g) sample of **11** dissolved in 10 mL of glyme was refluxed with 0.6 mmol (0.672 g) of DABCO for 12 h. The solvent was vacuum evaporated and the residue separated by TLC (CH_3CN) to give a single blue band (R_f 0.1) of the oily blue product, 1-(η^5-C_5H_5)-2-$NMe_2(CH_2)_2$-*closo*-1,2,3,4-$FeC_3B_7H_9$ (**12**), in 97% yield (0.009 g, 0.029 mmol). For **12**: HRMS calcd for $^{12}C_{12}{}^1H_{24}{}^{11}B_7{}^{14}N^{56}Fe$ 315.1909, found 315.1919; IR (KBr, cm^{-1}) 3364 (s), 2962 (s), 2928 (s), 2549 (s), 2366 (w), 2354 (w), 1731 (w), 1652 (m), 1567 (m), 1462 (m), 1415 (m), 1360 (w), 1260 (s), 1093 (s), 801 (s), 687 (m).

Crystallographic Data for Compounds 5, 7, 9, and 11. Single crystals of 1-(η^5-C_5H_5)-2-$NC(CH_2)_4$-*closo*-1,2,3,4-$FeC_3B_7H_9$, (**5**) (UPenn No. 3159), 1-(η^5-C_5H_5)-2-[(*p*-BrC_6H_4)(Me_3SiO)CH]-*closo*-1,2,3,4-$FeC_3B_7H_9$, (**7**) (UPenn No. 3162), 1-(η^5-C_5H_5)-2-$C_{14}H_{11}$-*closo*-1,2,3,4-$FeC_3B_7H_9$ (**9**) (UPenn No. 3185), and 1-(η^5-C_5H_5)-2-$H_3BNMe_2(CH_2)_2$-*closo*-1,2,3,4-$FeC_3B_7H_9$ (**11**) (UPenn No. 3177) were grown via slow evaporation from CH_2Cl_2 or 50:50 hexanes:CH_2Cl_2 in air.

Collection and Reduction of the Data. X-ray intensity data for **5**, **7**, **9**, and **11** were collected on a Rigaku R-AXIS IIc area detector employing graphite-monochromated Mo Kα radiation. Indexing was performed from a series of oscillation angles. A hemisphere of data

(7) Evans, D. A.; Truesdale, L. K.; Carroll, G. L. *J. Chem. Soc., Chem. Commun.* **1973**, 55−56.

Table 2. Crystallographic Data Collection and Structure Refinement Information

	5	**7**	**9**	**11**
empirical formula	$FeC_{13}B_7H_{22}N$	$FeC_{18}B_7H_{28}SiOBr$	$FeC_{22}B_7H_{25}$	$FeC_{12}B_8H_{27}N$
fw	323.84	499.92	420.94	327.68
crystal class	monoclinic	monoclinic	triclinic	monoclinic
space group	$P2_1/c$	$P2_1/c$	$P1$	$P2_1/c$
Z	4	4	2	4
a, Å	8.0275(1)	13.0327(3)	11.304(2)	12.8071(1)
b, Å	9.5860(1)	7.7587(1)	13.901(3)	6.5162(1)
c, Å	21.2344(4)	22.6750(6)	7.5662(14)	21.0254(2)
α, deg			105.688(8)	
β, deg	95.635(1)	100.783(1)	109.808(13)	95.785(1)
γ, deg			100.35(2)	
V, Å^3	1626.13(4)	2252.34(8)	1027.5(3)	1745.71(3)
μ, cm^{-1}	9.15	25.05	7.41	8.52
crystal size, mm	0.32 × 0.18 × 0.02	0.40 × 0.08 × 0.06	0.24 × 0.20 × 0.003	0.38 × 0.18 × 0.06
D_{calc}, g/cm^3	1.323	1.474	1.361	1.247
F(000)	672	1016	436	688
radiation	Mo Kα	Mo Kα	Mo Kα	Mo Kα
2θ angle, deg	5.1−50.7	5.28−50.7	5.8−50.76	5.28−50.7
temp, K	210	210	200	200
hkl collected	$-9 \le h \le 9$, $-11 \le k \le 11$, $-25 \le l \le 25$	$-15 \le h \le 15$, $-8 \le k \le 9$, $-27 \le l \le 27$	$-13 \le h \le 13$, $-16 \le k \le 16$, $-9 \le l \le 9$	$-15 \le h \le 15$, $-7 \le k \le 7$, $-25 \le l \le 24$
no. of reflns measd	13047	16434	8252	13517
no. of unique reflns	2958 (R_{int} = 0.0370)	4074 (R_{int} = 0.0424)	5746 (R_{int} = 0.0519)	3145 (R_{int} = 0.0348)
no. of observed reflns ($F > 4\sigma$)	2758	3712	5292	2975
no. of reflns used in refinement	2958	4074	5746	3145
no. of parameters	267	374	542	307
R^a indices ($F > 4\sigma$)	R_1 = 0.0390	R_1 = 0.0481	R_1 = 0.0607	R_1 = 0.0417
	wR_2 = 0.0844	wR_2 = 0.0843	wR_2 = 0.1547	wR_2 = 0.0944
R^a indices (all data)	R_1 = 0.0437	R_1 = 0.0563	R_1 = 0.0666	R_1 = 0.0451
	wR_2 = 0.0867	wR_2 = 0.0877	wR_2 = 0.1616	wR_2 = 0.0965
GOF^b	1.104	1.168	1.081	1.130
final difference peaks, e/Å^3	+0.203, −0.456	+0.276, −0.460	+0.507, −0.534	+0.208, −0.509

^{a} $R_1 = \sum||F_o| - |F_c||/\sum|F_o|$; $wR_2 = \{\sum w(F_o^2 - F_c^2)^2/\sum w(F_o^2)^2\}^{1/2}$. ^{b} GOF = $\{\sum w(F_o^2 - F_c^2)^2/(n - p)\}^{1/2}$ where n = no. of reflections; p = no. of parameters refined.

was collected using 8° oscillation angles for **5**, 5° oscillation angles for **7**, 6° oscillation angles for **9** and **11**, and a crystal-to-detector distance of 82 mm. Exposure times of 200 s (**5**), 300 s (**7**), 1000 s (**9**), and 300 s (**11**) were employed. Oscillation images were processed using bioteX,[8] producing a listing of unaveraged F^2 and $\sigma(F^2)$ values which were then passed to the teXsan program[9] package for further processing and structure solution on a Silicon Graphics Indigo R4000 computer. The intensity data were corrected for Lorentz and polarization effects, but not for absorption.

Solution and Refinement of the Structures. The structure was solved by direct methods (SIR92[10]). Refinement was by full-matrix least squares based on F^2 using SHELXL-93.[11] All reflections were used during refinement (F^2 values that were experimentally negative were replaced by $F^2 = 0$). Data collection and structure refinement information is given in Table 2.

Results and Discussions

We have previously shown[1] that the 6-CH_3-*nido*-5,6,9-$C_3B_7H_9^-$ (**1**$^-$) monoanion can be synthesized in excellent yields (eq 1) by a process (Figure 1) involving the initial nucleophilic attack of the *arachno*-4,6-$C_2B_7H_{12}^-$ anion at the nitrile carbon of acetonitrile, followed by nitrile reduction, deamination, and monocarbon insertion.

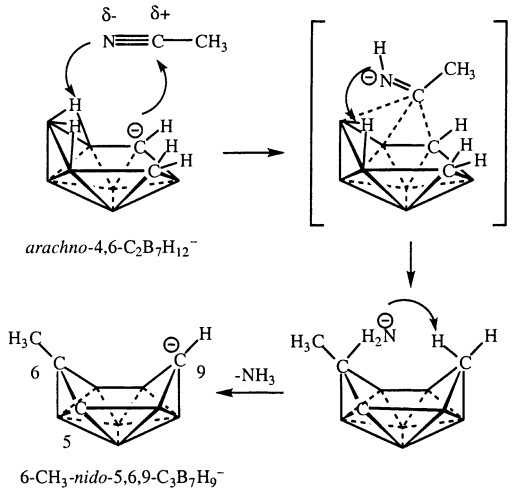

Figure 1. Previously proposed reaction sequence for the synthesis of 6-CH_3-*nido*-5,6,9-$C_3B_7H_9^-$ from the reaction of *arachno*-4,6-$C_2B_7H_{12}^-$ with CH_3CN.

$$Li^+arachno\text{-}4,6\text{-}C_2B_7H_{12}^- + CH_3CN \rightarrow Li^+(6\text{-}CH_3\text{-}nido\text{-}5,6,9\text{-}C_3B_7H_9^-) + NH_3 \quad (1)$$

We have now found that similar reactions with a variety of nitriles lead to the formation of substituted 6-R-*nido*-5,6,9-$C_3B_7H_9^-$ anions. The reactions with PhCN, $NC(CH_2)_4CN$,

(8) *bioteX: A suite of Programs for the Collection, Reduction and Interpretation of Imaging Plate Data*; Molecular Structure Corporation: 1995.
(9) *teXsan: Crystal Structure Analysis Package*; Molecular Structure Corporation: 1985 and 1992.
(10) SIR92: Altomare, A.; Burla, M. C.; Camalli, M.; Cascarano, M.; Giacovazzo, C.; Guagliardi, A.; Polidoro, G. *J. Appl. Crystallogr.* **1994**, *27*, 435.
(11) Sheldrick, G. M. *SHELXL-93: Program for the Refinement of Crystal Structures*; University of Göttingen: Göttingen, Germany, 1993.

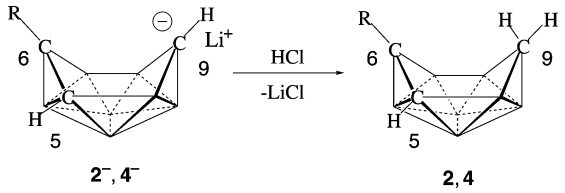

Figure 2. Protonation reactions of $\mathbf{2}^-$ and $\mathbf{4}^-$.

and [(*p*-BrC_6H_4)(Me_3SiO)CH]CN proceeded in a straightforward manner to give the Li^+(6-Ph-*nido*-5,6,9-$C_3B_7H_9^-$) ($\mathbf{2}^-$), Li^+(6-$NC(CH_2)_4$-*nido*-5,6,9-$C_3B_7H_9^-$) ($\mathbf{4}^-$), and Li^+-(6-[(*p*-BrC_6H_4)(Me_3SiO)CH]-*nido*-5,6,9-$C_3B_7H_9^-$) ($\mathbf{6}^-$) tricarbadecaboranyl anions. Typical isolated yields for $Li^+\mathbf{2}^-$ and $Li^+\mathbf{4}^-$ products were in the 74−80% range, but, most likely due to its larger steric demands, lower yields (35%) were found for $Li^+\mathbf{6}^-$. As can be seen in Table 1 for $\mathbf{2}^-$ and $\mathbf{4}^-$, the ^{11}B NMR spectra for each of the substituted tricarbadecaboranyl anions have a seven-line pattern essentially identical to that reported for 6-CH_3-*nido*-5,6,9-$C_3B_7H_9^-$.[1] The peak positions in $\mathbf{2}^-$ are shifted slightly downfield, which is consistent with the electron withdrawing nature of a Ph group compared to the Me group in $\mathbf{1}^-$.

As shown in Figure 2, the neutral compounds 6-Ph-*nido*-5,6,9-$C_3B_7H_{10}$ (**2**) and 6-$NC(CH_2)_4$-*nido*-5,6,9-$C_3B_7H_{10}$ (**4**) were prepared by reacting $\mathbf{2}^-$ and $\mathbf{4}^-$ with HCl. The ^{11}B NMR spectra of both **2** and **4** show seven different doublets at chemical shifts nearly identical to that observed for 6-CH_3-*nido*-5,6,9-$C_3B_7H_{10}$ (**1**).[1] Their ^{1}H NMR spectra show, in addition to the resonances of their respective phenyl and methylene substituents, three cage CH resonances. As in 6-CH_3-*nido*-5,6,9-$C_3B_7H_{10}$, one of the CH resonances in the spectra of both **2** and **4** appears at a high-field shift characteristic of an *endo*-CH hydrogen (**2**, −1.21 ppm; **4**, −1.52 ppm).[12] This is consistent with the protonations of $\mathbf{2}^-$ and $\mathbf{4}^-$ occurring, as was observed for 6-CH_3-*nido*-5,6,9-$C_3B_7H_9^-$, at the *endo*-positions of their C9 carbons. The two remaining cage CH resonances in both compounds appear at lower field (*exo*-C9H, 3.94 (**2**) and 3.25 (**4**) ppm; and C5H, 1.97 (**2**) and 1.85 (**4**) ppm). The room-temperature proton-decoupled ^{13}C NMR spectra of both compounds show, in addition to their substituent resonances, three broad resonances corresponding to three cage carbons.

As illustrated in eq 2, ferratricarbadecaboranyl analogues of ferrocene, including both bis-cage, $(CH_3{-}C_3B_7H_9)_2Fe$, and mixed-ligand, (η^5-C_5H_5)Fe($CH_3{-}C_3B_7H_9$), complexes, have been shown to result from the reactions of 6-CH_3-*nido*-5,6,9-$C_3B_7H_9^-$ ($\mathbf{1}^-$) with (η^5-C_5H_5)$Fe(CO)_2I$.[2a]

$$(\eta^5\text{-}C_5H_5)Fe(CO)_2I + Li^+(6\text{-}CH_3\text{-}nido\text{-}5,6,9\text{-}C_3B_7H_9^-) \xrightarrow[\mathbf{1}^-]{-LiI,\ -2CO} 1\text{-}(\eta^5\text{-}C_5H_5)\text{-}2\text{-}CH_3\text{-}closo\text{-}1,2,3,4\text{-}FeC_3B_7H_9 + 1\text{-}(\eta^5\text{-}C_5H_5)\text{-}4\text{-}CH_3\text{-}closo\text{-}1,2,3,4\text{-}FeC_3B_7H_9 + commo\text{-}Fe\text{-}(5\text{-}CH_3\text{-}closo\text{-}1,2,3,5\text{-}FeC_3B_7H_9) (4\text{-}CH_3\text{-}closo\text{-}1,2,3,4\text{-}FeC_3B_7H_9) \quad (2)$$

Similar reactions (eq 3) have now been used to prepare functionalized metallatricarbadecaborane complexes.

$$(\eta^5\text{-}C_5H_5)Fe(CO)_2I + Li^+(6\text{-}R\text{-}nido\text{-}5,6,9\text{-}C_3B_7H_9^-) \xrightarrow[\mathbf{2}^-,\ \mathbf{4}^-,\ \mathbf{6}^-]{-LiI,\ -2CO} 1\text{-}(\eta^5\text{-}C_5H_5)\text{-}2\text{-}R\text{-}closo\text{-}1,2,3,4\text{-}FeC_3B_7H_9 \quad (3)$$
3, **5**, **7**

Reactions employing 6-CH_3-*nido*-5,6,9-$C_3B_7H_9^-$ usually result in a skeletal rearrangement to produce isomeric side products, such as the 1-(η^5-C_5H_5)-4-CH_3-*closo*-1,2,3,4-$FeC_3B_7H_9$ complex in eq 2, where the methyl is attached at the 4-position carbon.[13] Likewise, bis-cage, $(CH_3{-}C_3B_7H_9)_2M$, side products are usually produced. On the other hand, in the reactions with $\mathbf{2}^-$, $\mathbf{4}^-$, and $\mathbf{6}^-$ (as well as the reactions of $\mathbf{8}^-$ and $\mathbf{10}^-$ discussed below) neither isomerization nor bis-cage $(R{-}C_3B_7H_9)_2Fe$ products were observed. In fact, as previously[2i] noted, even reactions intentionally designed to produce bis-cage complexes from the 6-Ph-*nido*-5,6,9-$C_3B_7H_9^-$ ($\mathbf{2}^-$) anion have been unsuccessful. The inability to form bis-cage complexes containing the functionalized monoanions is most probably a result of the unfavorable steric interactions that would occur between the bulky substituents on the two cages of such a complex. Thus, because other products are not produced, reactions with the new functionalized anions provide a more efficient route to mixed ligand metallatricarbadecaboranyl complexes than those reactions employing the 6-CH_3-*nido*-5,6,9-$C_3B_7H_9^-$ anion.

All ferratricarbadecaboranyl complexes were isolated as air-stable solids and were purified by TLC. Their compositions were established by mass spectrometry and elemental analyses.

The ^{11}B NMR spectra of **5** and **7** (and of **9** and **11** discussed below) are each consistent with C_1 cage symmetries and are similar to that previously reported for **3**[2g,i] and 1-(η^5-C_5H_5)-2-CH_3-*closo*-1,2,3,4-$FeC_3B_7H_9$.[2a] The ^{1}H NMR spectra of these compounds are likewise similar to that of 1-(η^5-C_5H_5)-2-CH_3-*closo*-1,2,3,4-$FeC_3B_7H_9$, each showing, in addition to the resonances arising from their C2 substituents, two CH resonances with one occurring at a low field shift (∼6.61 to 6.04 ppm) characteristic of the proton attached to the low-coordinate C3 carbon, and the other at a high field shift (>1.83 ppm) characteristic of the C4H proton.

(12) (a) Plesek, J.; Hermánek, S.; Janousek, Z. *Collect. Czech. Chem. Commun.* **1977**, *42*, 785−792. (b) Tebbe, F. N.; Garrett, P. M.; Hawthorne, M. F. *J. Am. Chem. Soc.* **1966**, *88*, 607−608. (c) Tebbe, F. N.; Garrett, P. M.; Hawthorne, M. F. *J. Am. Chem. Soc.* **1968**, *90*, 869−879. (d) Stibr, B.; Plesek, J.; Hermánek, S. *Chem. Ind.* **1972**, *19*, 649. (e) Stibr, B.; Base, K.; Hermánek, S.; Plesek, J. *J. Chem. Soc., Chem. Commun.* **1976**, 150−151. (f) Base, K.; Hermánek, S.; Stibr, B. *Chem. Ind.* **1976**, *18*, 1068−1069. (g) Base, K.; Hermánek, S.; Hanousek, F. *J. Chem. Soc., Chem. Commun.* **1984**, 299. (h) Janousek, Z.; Plesek, J.; Hermánek, S.; Stibr, B. *Polyhedron* **1985**, *4*, 1797−1798. (i) Stibr, B.; Janousek, Z.; Plesek, J.; Jelinek, T.; Hermánek, S. *J. Chem. Soc., Chem. Commun.* **1985**, 1365−1366. (j) Jelinek, T.; Hermánek, S.; Stibr, B.; Plesek, J. *Polyhedron* **1986**, *5*, 1303−1305. (k) Stibr, B.; Plesek, J.; Jelinek, T.; Hermánek, S.; Solntsev, K. A.; Kuznetsov, N. T. *Collect. Czech. Chem. Commun.* **1987**, *52*, 957−959.

(13) Plumb, C. A.; Sneddon, L. G. *Organometallics* **1992**, *11*, 1681−1685.

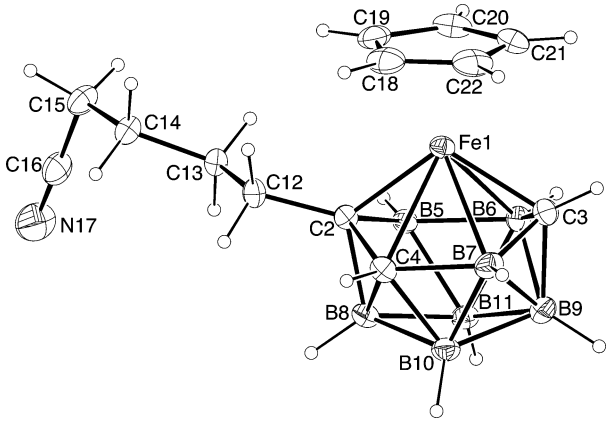

Figure 3. ORTEP drawing of the structure of 1-(η^5-C_5H_5)-2-NC$(CH_2)_4$-*closo*-1,2,3,4-$FeC_3B_7H_9$ (**5**). Important intracage distances are given in Table 3. Other selected distances (Å) and angles (deg): C2−C12, 1.524(3); C16−N17, 1.139(4); C12−C2−B8, 115.7(2); C15−C16−N17, 178.3(3); Fe1−C2−C12, 126.4(2); C2−Fe1−C3, 111.17(10).

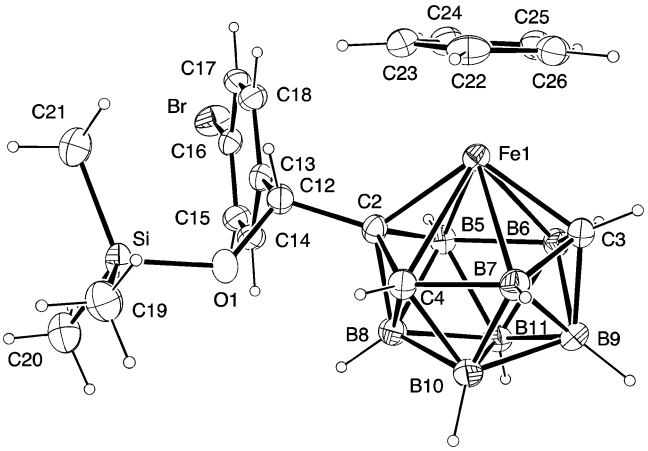

Figure 4. ORTEP drawing of the structure of 1-(η^5-C_5H_5)-2-[(*p*-BrC_6H_4)(Me_3SiO)CH]-*closo*-1,2,3,4-$FeC_3B_7H_9$ (**7**). Important intracage distances are given in Table 3. Other selected distances (Å) and angles (deg): C2−C12, 1.544(5); C12−O1, 1.413(4); Si−O1, 1.657(3); C12−C2−B8, 115.6(3); Fe1−C2−C12, 126.4(3); C2−Fe1−C3, 110.4(2); C2−C12−O1, 108.0(3); C2−C12−C13, 112.1(3); Si−O1−C12, 128.4(2).

In agreement with both the spectroscopic data and the previous structural determinations of 1-(η^5-C_5H_5)-2-CH_3-*closo*-1,2,3,4-$FeC_3B_7H_9$[2a] and 1-(η^5-C_5H_5)-2-Ph-*closo*-1,2,3,4-$FeC_3B_7H_9$[2g,i] (**3**), crystallographic determinations of 1-(η^5-C_5H_5)-2-NC$(CH_2)_4$-*closo*-1,2,3,4-$FeC_3B_7H_9$ (**5**) (Figure 3) and 1-(η^5-C_5H_5)-2-[(*p*-BrC_6H_4)(Me_3SiO)CH]-*closo*-1,2,3,4-$FeC_3B_7H_9$ (**7**) (Figure 4) confirm that the metal atoms in these complexes are η^6-coordinated to the puckered six-membered face of the tricarbadecaboranyl cage with the functional groups bonded to the C2 cage carbon adjacent to the metal. Thus, these complexes can be considered as mixed ligand analogues of ferrocene in which a formal Fe^{2+} ion is sandwiched between tricarbadecaboranyl and cyclopentadienyl monoanions. From a cluster point of view,[14] the 11-vertex $FeC_3B_7H_9$ fragment has a *closo* skeletal electron count (24 skeletal electrons, with the (η^5-C_5H_5)Fe group donating 1 skeletal electron) and it, therefore, adopts the octadecahedral structure normally observed for such systems.

Table 3. Selected Intramolecular Distances (Å) in **3**, **5**, **7**, **9**, and **11**

bond	**3**[a]	**5**	**7**	**9**[b]	**11**
Fe−C2	1.982(2)	1.980(2)	1.991(4)	1.970(8)	1.980(2)
Fe−C3	1.955(3)	1.956(3)	1.954(4)	1.957(8)	1.959(3)
Fe−C4	2.258(3)	2.244(2)	2.282(4)	2.244(8)	2.250(2)
Fe−B5	2.239(3)	2.245(3)	2.224(4)	2.238(7)	2.241(3)
Fe−B6	2.253(3)	2.239(3)	2.227(4)	2.253(8)	2.241(3)
Fe−B7	2.275(3)	2.265(3)	2.292(4)	2.287(9)	2.283(3)
Fe−Cp	1.695(3)	1.686(3)	1.694(5)	1.692(7)	1.688(2)
C2−C4	1.502(4)	1.500(3)	1.500(4)	1.509(11)	1.497(3)
C4−B7	1.750(4)	1.747(4)	1.746(5)	1.749(13)	1.746(4)
B7−C3	1.576(4)	1.574(4)	1.558(5)	1.579(13)	1.568(4)
C3−B6	1.578(4)	1.580(4)	1.588(5)	1.576(11)	1.578(4)
B6−B5	1.841(5)	1.843(4)	1.846(6)	1.846(12)	1.854(4)
B5−C2	1.593(4)	1.586(3)	1.584(5)	1.589(9)	1.594(4)

[a] Taken from ref 2i. [b] Since there were no significant differences, bond distances for only one of the two independent molecules found in the asymmetric unit of **9** are given.

Selected intracage distances for **3**, **5**, and **7** (and **9** and **11**) are compared in Table 3. In each case, the metal is approximately centered over the puckered six-membered open face, with the closest metal−cage interactions being with the two carbons, C2 and C3, which are puckered out of the ring. Longer and approximately equivalent bond lengths are observed between the metals and the remaining four atoms (C4, B5, B6, and B7) on the tricarbadecaboranyl bonding face. The M−C2 and M−C3 bond lengths in these complexes are significantly shorter than the M−C bond lengths found to the ring carbons in their cyclopentadienyl (∼2.05 to 2.07 Å) ligands. As previously noted,[15] the orbitals on the open face of even a planar polyhedral cluster are orientated more directly toward the metal than in a cyclopentadienyl ring. This enhances the overlap of the metal and ligand orbitals and strengthens the bonding. In the case of the tricarbadecaboranyl cages, the puckered ring structure allows even stronger interactions of the metal with the C2 and C3 carbons.

Regardless of the substituent at the C2 carbon, the Fe−C2 distances (**3**, 1.982(2) Å; **5**, (1.980(2) Å; **7**, 1.991(4) Å) were found to be considerably longer than their corresponding Fe−C3 distances (**3**, 1.955(3) Å; **5**, 1.956(3) Å; **7**,1.954-(4) Å, respectively). In complexes **3** and **5**, the plane of the η^5-C_5H_5 ring is reasonably parallel to the C4−B5−B6−B7 plane, but, consistent with the longer Fe−C2 distance in **7** relative to those in **3** and **5**, in **7** these planes have a dihedral angle of 8.3(9)° such that the η^5-C_5H_5 group is tilted away from the bulky (*p*-BrC_6H_4)(Me_3SiO)CH− substituent.

The reaction (Figure 5) of *arachno*-4,6-$C_2B_7H_{12}^-$ with cyanoanthracene was expected to provide a route to an anthracene-substituted ferratricarbadecaboranyl complex. However, a structural characterization of the final product revealed that, during the course of the reaction, anthracene reduction occurred to produce the dihydroanthracene (DHA)

(14) (a) Wade, K. *Adv. Inorg. Chem. Radiochem.* **1976**, *18*, 1−66. (b) Williams, R. E. *Adv. Inorg. Chem. Radiochem.* **1976**, *18*, 67−142. (c) Williams, R. E. *Chem. Rev.* **1992**, *92*, 117−201. (d) Williams, R. E. In *Electron Deficient Boron and Carbon Clusters*; Olah, G. A., Wade, K., Williams, R. E., Eds.; Wiley: New York, 1991.

(15) (a) Hawthorne, M. F.; Young, D. C.; Andrews, T. D.; Howe, D. V.; Pilling, R. L.; Pitts, A. D.; Reintjes, M.; Warren, L. F., Jr.; Wegner, P. A. *J. Am. Chem. Soc.* **1968**, *90*, 879−896. (b) Calhorda, M. J.; Mingos, D. M. P.; Welch, A. *J. Organomet. Chem.* **1982**, *228*, 309−320. (c) Mingos, D. M. P. *J. Chem. Soc., Chem. Commun.* **1977**, 602−610.

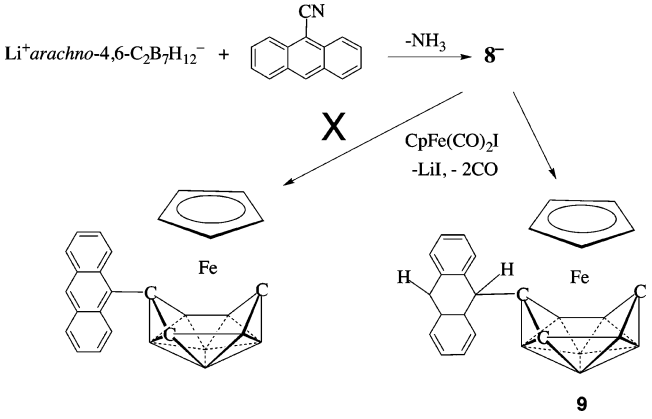

Figure 5. Reaction of $\mathbf{8}^-$ with (η^5-C_5H_5)Fe(CO)$_2$I.

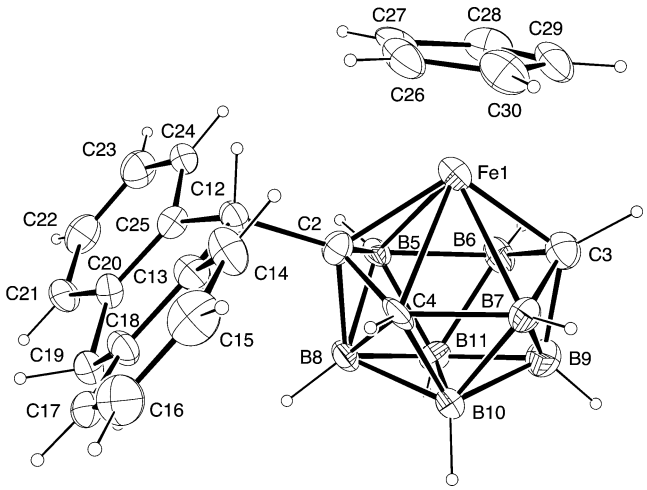

Figure 6. ORTEP drawing of the structure of one of the two independent molecules in the unit cell of 1-(η^5-C_5H_5)-2-$C_{14}H_{11}$-*closo*-1,2,3,4-$FeC_3B_7H_9$ (**9**). Important intracage distances are given in Table 3. Other selected distances (Å) and angles (deg): C2−C12, 1.578(9); C12−C25, 1.515(9); C25−C20, 1.377(11); C18−C19, 1.500(10); C18−C13, 1.388(11); C13−C12, 1.518(9); C19−C20, 1.509(10); C20−C21, 1.420(10); C21−C22, 1.389(12); C22−C23, 1.354(13); C23−C24, 1.396(11); C24−C25, 1.423(10); C13−C14, 1.432(10); C14−C15, 1.411(12); C15−C16, 1.372(14); C16−C17, 1.372(11); C17−C18, 1.399(10); C12−C2−B8, 114.9(6); C12−C2−Fe1, 127.5(5); C2−Fe1−C3, 111.5(3); C2−C12−C13, 112.1(6); C2−C12−C25, 111.2(5); C13−C12−C25, 112.6(6); C18−C19−C20, 114.2(7); C19−C20−C25, 122.4(7); C20−C25−C12, 121.5(6); C18−C13−C12, 122.1(6); C19−C18−C13, 121.4(6).

substituted product 1-(η^5-C_5H_5)-2-$C_{14}H_{11}$-*closo*-1,2,3,4-$FeC_3B_7H_9$ (**9**). As can be seen in the ORTEP drawing in Figure 6, hydrogenation of the central ring occurred and, as a result, the tetrahedral C12 and C19 carbons are puckered out of the C13−C18−C20−C25 plane, such that the central ring adopts a boat conformation with the ferratricarbaboranyl fragment bound at the axial position of the C12 ring carbon. Accordingly, the planes of the C13−C14−C15−C16−C17−C18 and C20−C21−C22−C23−C24−C25 rings no longer lie in the C13−C18−C20−C25 plane, forming 8(1)° and 7(1)° dihedral angles with that plane. These dihedral angles, as well as the distances and angles observed for the central ring, are consistent with those that have been observed in dihydroanthracene[16] and its derivatives.[17] The degree of nonplanarity of the central ring can be expressed by the sum of the six torsional angles of the six carbons within the central ring (for a planar ring this sum would be 0°).[17a] The 81.5°

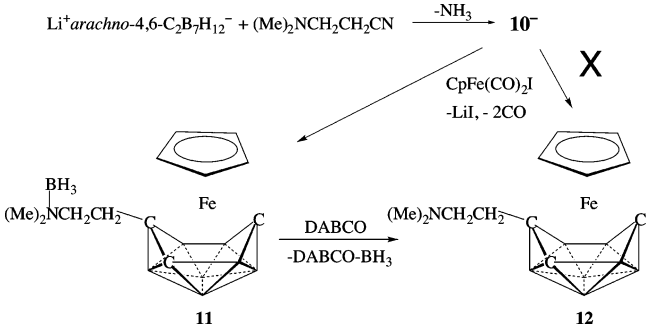

Figure 7. Reaction of $\mathbf{10}^-$ with (η^5-C_5H_5)Fe(CO)$_2$I.

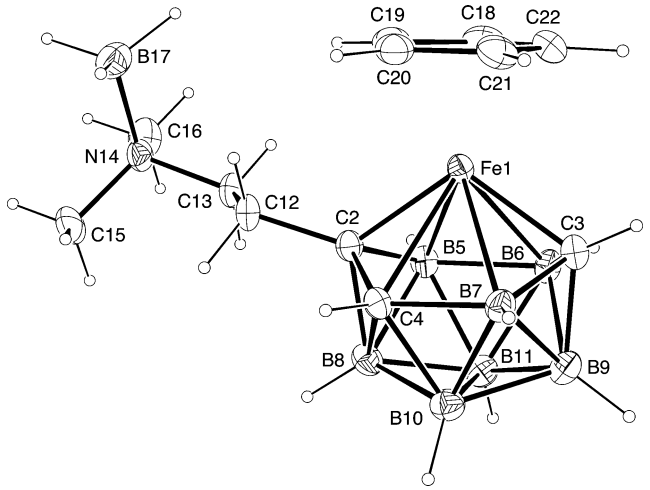

Figure 8. ORTEP drawing of the structure of 1-(η^5-C_5H_5)-2-H_3BNMe_2-$(CH_2)_2$-*closo*-1,2,3,4-$FeC_3B_7H_9$ (**11**). Important intracage distances are given in Table 3. Other selected distances (Å) and angles (deg): C2−C12, 1.525(3); B17−N14, 1.620(4); C13−N14, 1.506(3); C15−N14, 1.484(4); C16−N14, 1.492(4); C12−C2−B8, 115.1(2); C12−C2−Fe1, 126.8(2); C2−Fe1−C3, 110.74(10); B17−N14−C13, 112.4(2); B17−N14−C15, 111.2-(3); B17−N14−C16, 108.4(2); C15−N14−C16, 108.4(2).

value (and 77.4° in the other independent molecule) found for the C12−C13−C18−C19−C20−C25 ring in **9** is similar to that found in 9-Me_3Si-10-Me-DHA (85.4°), but much smaller than those found for the more distorted 9-Me-DHA (136.4°) and 9-Me_3Si-DHA (121.5°) derivatives.[17a] The intracage distances (Table 3) and angles are consistent with those observed for the other ferratricarbaboranes.

As can be seen in Figure 7, the reaction of *arachno*-4,6-$C_2B_7H_{12}^-$ and $Me_2NCH_2CH_2CN$ was expected to provide a route to the complex 1-(η^5-C_5H_5)-2-$NMe_2(CH_2)_2$-*closo*-1,2,3,4-$FeC_3B_7H_9$ (**12**), which would have a dimethylamine group tethered to the cage. Surprisingly, as shown in the ORTEP drawing in Figure 8, a crystallographic determination established that the final product was instead the complex 1-(η^5-C_5H_5)-2-$BH_3NMe_2(CH_2)_2$-*closo*-1,2,3,4-$FeC_3B_7H_9$ (**11**) containing a BH_3-coordinated amine. Given the low yields observed for the formation of **11** (7% from *arachno*-4,6-$C_2B_7H_{12}^-$), the BH_3 group was undoubtedly generated by

(16) Herbstein, F. H.; Kapon, M.; Reisner, G. M. *Acta Crystallog., Sect B* **1986**, *42*, 181−187.

(17) (a) Dhar, R. J.; Sygula, A.; Fronczek, F. R.; Rabideau, P. W. *Tetrahedron* **1992**, *48*, 9417−9426. (b) Brennan, T.; Putkey, E. F.; Sundaralingam, *J. Chem. Soc., Chem. Commun.* **1971**, 1490−1491. (c) Bordner, J.; Stanford, R. H., Jr.; Ziegler, H. E. *Acta Crystallog., Sect B* **1973**, *29*, 313−318. (d) Leory, F.; Courseille, C.; Daney, M.; Bouas-Laurent, H. *Acta Crystallog., Sect B* **1976**, *32*, 2792−2796.

cage decomposition reactions during the course of the reaction. The B−N distance of 1.620(4) Å in **11** is similar to the values that have been found in other amine−boranes,[18] and the intracage distances (Table 3) and angles are likewise consistent with those of the other ferratricarbadecaboranyl complexes reported above. In agreement with the structural determination, the ^{11}B NMR of **11** contains, in addition to the seven cage-boron resonances observed for complexes **3**, **5**, **7**, and **9**, an eighth resonance at −9.8 ppm that can be assigned to the amine-coordinated BH_3.

As shown in Figure 7, removal of the BH_3 group from **11** to produce the 1-(η^5-C_5H_5)-2-$NMe_2(CH_2)_2$-*closo*-1,2,3,4-$FeC_3B_7H_9$ (**12**) complex containing the free amine group was achieved by reaction of **11** with DABCO (triethylenediamine). Although **12** was not crystallographically characterized, the removal of the borane was confirmed by both mass spectrometry and ^{11}B NMR. Thus, instead of the eight resonances observed for **11**, the ^{11}B NMR spectrum of **12** exhibited only the seven cage-boron resonances.

To summarize, this paper demonstrates both a general route to 6-R-*nido*-5,6,9-$C_3B_7H_9^-$ anions via the reactions of *arachno*-4,6-$C_2B_7H_{12}^-$ with nitriles and that the new tricarbadecaboranyl anions can then be used to generate functionalized metallatricarbadecaboranyl complexes containing a wide range of organic substituents. These pathways now provide great flexibility for the systematic tuning of the chemical and bioactivity properties of metallatricarbadecaborane complexes.

Acknowledgment. We thank the National Science Foundation for the support of this research.

Supporting Information Available: X-ray crystallographic data for structure determinations of compounds **5**, **7**, **9**, and **11** (CIF). This material is available free of charge via the Internet at http://pubs.acs.org.

IC049827A

(18) Buhl, M.; Steinke, T.; Schleyer, P. v. R.; Boese, R. *Angew. Chem., Int. Ed. Engl.* **1991**, *30*, 1160−1161.